ELSEVIER

Journal of Quantitative Spectroscopy & Radiative Transfer 90 (2005) 343–366

Journal of Quantitative Spectroscopy & Radiative Transfer

www.elsevier.com/locate/jqsrt

Polarization of line radiation in the presence of external electric quadrupole and uniform magnetic fields: II. Arbitrary orientation of magnetic field

Yee Yee Oo[a], K.N. Nagendra[b], Sharath Ananthamurthy[a], Swarnamala Sirsi[c], R. Vijayashankar[d], G. Ramachandran[b,*]

[a] *Department of Physics, Bangalore University, Bangalore 560 056, India*
[b] *Indian Institute of Astrophysics, Bangalore 560 034, India*
[c] *Yuvaraja's College, University of Mysore, Mysore 570 005, India*
[d] *Department of Physics, Oklahoma State University, Stillwater, OK 74078-3072, USA*

Received 6 October 2003; accepted 11 April 2004

Abstract

In continuation of our earlier investigation (referred to hereafter as part I) where we considered the mathematically simple case of magnetic field orientation along the Z-axis of the principal axes frame (PAF) of the electric quadrupole field, we take up here the general problem of arbitrary orientation of the magnetic field with respect to the PAF, and investigate the nature of polarized line spectra of an atom making a transition from an upper level with spin J_u to a lower level with spin J_l. Explicit formulae for the emitted Stokes parameters are obtained and we discuss their physical significance by computing numerically the cases of transitions $J_u = 1 \to J_l = 0$ and $J_u = \frac{3}{2} \to J_l = \frac{1}{2}$. Specific features or signatures of the polarized line spectra are discussed as functions of the relevant physical parameters. The Stokes parameters are also analyzed in terms of the Zeeman term contributions and the cross-term contributions (which arise due to quantum interference).

Keywords: Polarization; Line formation; Quadrupole electric field; Magnetic field

1. Introduction

The rapid strides witnessed in astrophysical spectropolarimetry in recent years have revealed a variety of details which have so far remained inaccessible. In this context, it is of interest to examine theoretically the nature of signatures in polarized line spectra which arise due to the possible presence of electric fields in addition to the well established presence of magnetic fields in astrophysical

* Corresponding author. Tel.: +91-80-2553-0672-0676; fax: +91-80-2553-4043/4019.
E-mail address: gr@iiap.res.in (G. Ramachandran).

0022-4073/$ - see front matter © 2004 Elsevier Ltd. All rights reserved.
doi:10.1016/j.jqsrt.2004.04.007

plasmas. In an earlier paper [1], hereafter referred to as part I, we discussed the polarization of radiation emitted by an atom making a transition from an upper level with spin-1 to a lower spin-0 level when the atom is exposed to an external electric quadrupole field. We have also examined in part I, the situation where a uniform magnetic field is present in addition to the electric quadrupole field. It was assumed that the magnetic field is oriented along the Z-axis of the principal axes frame (PAF) of the electric quadrupole field (see part I for a definition of PAF). This particular geometry was chosen in that paper for the sake of mathematical simplicity of the problem. We have indicated that the theoretical calculations presented in part I may also find application in the context of cloud physics. Oxygen has a prominent line at 844.6 nm corresponding to a spin-1 to spin-0 transition, while Nitrogen has a prominent line at 868.6 nm which corresponds to a transition from a spin-$\frac{3}{2}$ to a spin-$\frac{1}{2}$ level. Recently, spectropolarimetric observations of the Na I 589 and 589.6 nm emission lines have been reported [2] from the exosphere of Mercury. As is well known, the 589 nm emission line corresponds to a transition from spin-$\frac{3}{2}$ to spin-$\frac{1}{2}$, whereas 589.6 nm line involves a transition from spin-$\frac{1}{2}$ to spin-$\frac{1}{2}$. It is interesting to note that the spin-$\frac{3}{2}$ level is sensitive to the electric quadrupole as well as uniform magnetic fields, whereas the spin-$\frac{1}{2}$ levels get split only due to the magnetic field. It is also known that the linear polarization pattern of these Na I lines, observed in solar spectra, still poses a theoretical challenge (see [3,4] for several papers concerning this important line). From the point of view of astrophysical applications, one may have to consider, in general, situations where the direction of magnetic field is arbitrary, and not necessarily along the Z-axis of the PAF. We study here theoretically, spin-$\frac{3}{2}$ to spin-$\frac{1}{2}$ and spin-1 to spin-0 transitions, in the combined presence of electric quadrupole and uniform magnetic fields, considering an arbitrary orientation of the magnetic field with respect to the PAF of the electric field.

As we have seen in part I, a spin-1 level splits into three levels which correspond, in general, to three orthonormal linear combinations of the $|1,\pm1\rangle$ and $|1,0\rangle$ states, when both the fields are present. Even in the case of a pure electric quadrupole field, the eigen states of energy are superposition of the $|1,m\rangle$ states, in contrast to the case of a pure magnetic field, where the energy eigen states are identical individually to the $|1,m\rangle$ states themselves. It is desirable, therefore, to develop a formalism to describe the polarization of line radiation emitted by the atom while it makes a transition from an upper level with spin J_{u} to a lower level with spin J_{l}, which is applicable to situations where the upper and lower levels are split, due to external fields, into $2J_{\mathrm{u}}+1$ levels $[|\Psi_i\rangle,\ i=1,2,\ldots,(2J_{\mathrm{u}}+1)]$ and $2J_{\mathrm{l}}+1$ levels $[|\Psi_f\rangle,\ f=1,2,\ldots,(2J_{\mathrm{l}}+1)]$ respectively, where $|\Psi_i\rangle$ and $|\Psi_f\rangle$ are not necessarily identifiable with the magnetic substates. In such scenarios, the polarization of the atomic states may conveniently be represented by the Fano statistical tensors. It is also well known that the Stokes parameters (I,Q,U,V) completely specify a general state of the polarized radiation. Using the density matrix formalism we derive elegant formulae in Section 2 for the emergent Stokes parameters in terms of the Fano statistical tensors t^k_q characterizing the upper and lower levels. These tensors t^k_q are governed completely by the details of the relative configuration of the electric and the magnetic fields. In Section 3, we derive explicit expressions for the Fano statistical tensors considering the particular cases of spin $J_{\mathrm{u}}=1$ as well as $J_{\mathrm{u}}=\frac{3}{2}$, when the atom is exposed to a combination of an electric quadrupole field together with a uniform magnetic field which is oriented in any arbitrary orientation with respect to the PAF. A spin $J_{\mathrm{l}}=\frac{1}{2}$ level is not susceptible to the electric quadrupole field and splits into two levels due to the magnetic field alone. Section 4 is devoted to a presentation of numerical results in some typical cases and a discussion of the theoretical results obtained in this paper.

2. General theory of the line polarization when both the upper and lower atomic levels are split by the presence of external fields

Using the same notations as in part I, we may express the upper (spin J_u) and lower (spin J_l) levels $|\Psi_i\rangle$ and $|\Psi_f\rangle$, with energy eigen values E_i, E_f, respectively, as

$$|\Psi_i\rangle = \sum_{m_u=-J_u}^{J_u} c^i_{m_u} |J_u, m_u\rangle, \quad i = 1, 2, \ldots, (2J_u + 1), \tag{1}$$

with $\sum_{m_u} |c^i_{m_u}|^2 = 1$ and

$$|\Psi_f\rangle = \sum_{m_l=-J_l}^{J_l} c^f_{m_l} |J_l, m_l\rangle, \quad f = 1, 2, \ldots, (2J_l + 1), \tag{2}$$

with $\sum_{m_l} |c^f_{m_l}|^2 = 1$.

The corresponding atomic spin density matrices ρ^i and ρ^f are, respectively, given, in terms of their elements, by

$$\begin{aligned}\rho^i_{m_u,m'_u} &= c^i_{m_u} c^{i*}_{m'_u} \\ &= \frac{1}{[J_u]^2} \sum_{k_u=0}^{2J_u} (-1)^{q_u} [k_u] t^{k_u}_{q_u}(i) C(J_u, k_u, J_u; m'_u, -q_u, m_u)\end{aligned} \tag{3}$$

and

$$\begin{aligned}\rho^f_{m_l,m'_l} &= c^f_{m_l} c^{f*}_{m'_l} \\ &= \frac{1}{[J_l]^2} \sum_{k_l=0}^{2J_l} (-1)^{q_l} [k_l] t^{k_l}_{q_l}(f) C(J_l, k_l, J_l; m'_l, -q_l, m_l),\end{aligned} \tag{4}$$

where the short-hand $[J] = (2J + 1)^{1/2}$ is used.

It may be noted that Eqs. (3) and (4) define the Fano statistical tensors $t^{k_u}_{q_u}(i)$ and $t^{k_l}_{q_l}(f)$ characterizing the spin polarization of the initial and final atomic states, once the expansion coefficients $c^i_{m_u} = \langle J_u, m_u | \Psi_i \rangle$ and $c^f_{m_l} = \langle J_l, m_l | \Psi_f \rangle$ are known. These coefficients $c^i_{m_u}$ and $c^f_{m_l}$ are obtained by diagonalizing the Hamiltonian H_{int}, characterizing the interaction of the atom with the external fields. This is explicitly demonstrated for spin-1 and spin-$\frac{3}{2}$ systems in the next section.

Let us denote by $\langle f | T(\mathbf{k}, \mu) | i \rangle$, the transition matrix element from the initial state $|\Psi_i\rangle$ to the final state $|\Psi_f\rangle$, when it is accompanied by the emission of radiation of frequency ω, momentum $\mathbf{k}$ in the direction (θ_k, ϕ_k) (see Fig. 1) and polarization $\mu = \pm 1$ corresponding to the left and right circular polarization states as defined by Rose [5]. The transition matrix element is readily given, following

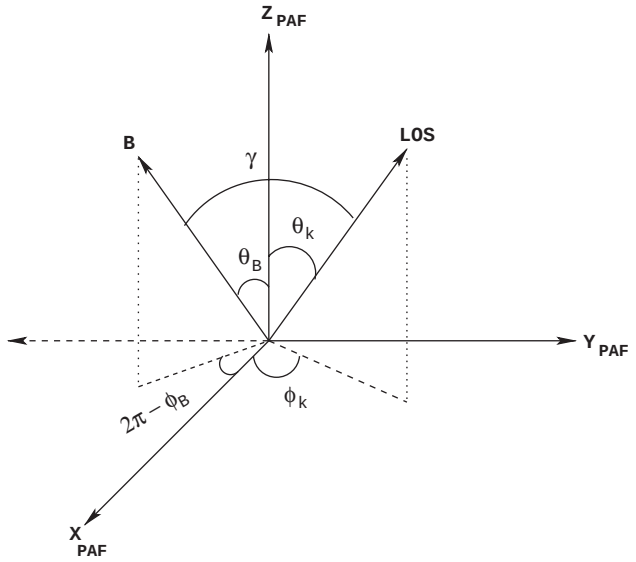

Fig. 1. The magnetic field **B** and the direction **k** of emission of radiation identified as LOS with reference to the PAF coordinate system. γ is the angle between the direction of the magnetic field and the line of sight.

part I, by

$$\langle f|T(\mathbf{k},\mu)|i\rangle = \frac{1}{(E_i - E_f - \omega) - \mathrm{i}(\Gamma_i + \Gamma_f)} \sum_{L=|J_\mathrm{u}-J_\mathrm{l}|}^{(J_\mathrm{u}+J_\mathrm{l})} (-\mathrm{i}\mu)^{h(L)} \mathscr{J}_L \times \sum_{m_\mathrm{u}=-J_\mathrm{u}}^{J_\mathrm{u}} \sum_{m_\mathrm{l}=-J_\mathrm{l}}^{J_\mathrm{l}} c^i_{m_\mathrm{u}} c^{f*}_{m_\mathrm{l}} C(J_\mathrm{l}, L, J_\mathrm{u}; m_\mathrm{l}, M, m_\mathrm{u}) \times D^L_{M,\mu}(\phi_k, \theta_k, -\phi_k)^*, \tag{5}$$

where Γ_i and Γ_f denote the natural widths of the levels $|\Psi_i\rangle$ and $|\Psi_f\rangle$ with energies E_i and E_f, while

$$\mathscr{J}_L = g(L)\mathscr{M}_L + h(L)\mathscr{E}_L \; g(L) = \frac{1}{2}\left[1 - \pi_u\pi_\mathrm{l}(-1)^L\right] \; h(L) = \frac{1}{2}\left[1 + \pi_u\pi_\mathrm{l}(-1)^L\right] \tag{6}$$

which indicate that the multipole transition strength $\mathscr{J}_L$ is either a magnetic transition $\mathscr{M}_L$, or an electric transition $\mathscr{E}_L$, when the atomic levels are good eigen states of parity. The $\Pi_\mathrm{u}, \Pi_\mathrm{l}$ denote the parities of upper and lower levels. The total angular momentum of the emitted radiation and its projection along the quantization axis parallel to Z-axis of PAF are denoted by L and M, respectively. The $D^L_{M,\mu}(\phi_k, \theta_k, -\phi_k)$ denote elements of the well-known Wigner rotation matrices, as defined in Rose [5].

The density matrix ρ^γ describing the state of polarization of the emitted radiation is then given in terms of its elements by

$$\rho^\gamma_{\mu,\mu'}(f,i) = \langle f|T(\mathbf{k},\mu)|i\rangle \, p_i \langle f|T(\mathbf{k},\mu')|i\rangle^*, \tag{7}$$

where p_i are given, under thermodynamic equilibrium conditions, by

$$p_i = P_u^{-1} \mathrm{e}^{-E_i/k_\mathrm{B}T}, \quad P_u = \sum_{i=1}^{(2J_\mathrm{u}+1)} \mathrm{e}^{-E_i/k_\mathrm{B}T}. \tag{8}$$

In the above equation P_u denotes the partition function, k_B the Boltzmann constant and T the temperature. Using Eq. (5), we may write Eq. (7) explicitly in the form

$$\begin{aligned}\rho^{\gamma}_{\mu,\mu'}(f,i) = p_i F(f,i;x) \sum_{L}\sum_{L'} (-\mathrm{i}\mu)^{h(L)} (\mathrm{i}\mu')^{h(L')} \mathscr{J}_L \mathscr{J}^*_{L'} \sum_{m_\mathrm{u},m_\mathrm{l}} \sum_{m'_\mathrm{u},m'_\mathrm{l}} c^i_{m_\mathrm{u}} c^{f\,*}_{m_\mathrm{l}} c^{i*}_{m'_\mathrm{u}} c^{f}_{m'_\mathrm{l}} \\ \times C(J_\mathrm{l}, L, J_\mathrm{u}; m_\mathrm{l}, M, m_\mathrm{u}) C(J_\mathrm{l}, L', J_\mathrm{u}; m'_\mathrm{l}, M', m'_\mathrm{u}) \\ \times D^{L}_{M,\mu}(\phi_k, \theta_k, -\phi_k)^* D^{L'}_{M',\mu'}(\phi_k, \theta_k, -\phi_k),\end{aligned} \tag{9}$$

where the unnormalized profile function

$$F(f,i;x) = \frac{1}{(E_i - E_0 - x\Gamma_{f,i})^2 + \Gamma^2_{f,i}}, \tag{10}$$

is written in terms of $x = (\omega - \omega_0)/\Gamma_{f,i}$, where $\omega_0 = E_0 - E_f$ denotes the conventional frequency displacement from the line center expressed in natural width units and $\Gamma_{f,i} = \Gamma_f + \Gamma_i$.

Observing from Eqs. (3) and (4) that

$$t^{k_\mathrm{u}}_{q_\mathrm{u}}(i) = [J_\mathrm{u}] \sum_{m_\mathrm{u}=-J_\mathrm{u}}^{J_\mathrm{u}} (-1)^{m_\mathrm{u}-J_\mathrm{u}} C(J_\mathrm{u}, J_\mathrm{u}, k_\mathrm{u}; m'_\mathrm{u}, -m_\mathrm{u}, q_\mathrm{u}) c^i_{m_\mathrm{u}} c^{i*}_{m'_\mathrm{u}}, \tag{11a}$$

$$t^{k_\mathrm{l}}_{q_\mathrm{l}}(f) = [J_\mathrm{l}] \sum_{m_\mathrm{l}=-J_\mathrm{l}}^{J_\mathrm{l}} (-1)^{m_\mathrm{l}-J_\mathrm{l}} C(J_\mathrm{l}, J_\mathrm{l}, k_\mathrm{l}; m'_\mathrm{l}, -m_\mathrm{l}, q_\mathrm{l}) c^f_{m_\mathrm{l}} c^{f\,*}_{m'_\mathrm{l}}, \tag{11b}$$

and making use of standard Racah algebra techniques, we may now express $\rho^{\gamma}_{\mu,\mu'}(f,i)$ in the elegant form

$$\rho^{\gamma}_{\mu,\mu'}(f,i) = \sum_{k_\mathrm{u}} \sum_{k_\mathrm{l}} \sum_{K=|k_\mathrm{u}-k_\mathrm{l}|}^{(k_\mathrm{u}+k_\mathrm{l})} ((t^{k_\mathrm{u}}(i) \otimes t^{k_\mathrm{l}}(f))^K . \mathscr{A}^K(\mu,\mu')). \tag{12}$$

In the above equation, the analyzing powers are given by

$$\begin{aligned}\mathscr{A}^K_{-Q}(\mu,\mu') = p_i F(f,i;x) \sum_{L,L'} (-\mathrm{i}\mu)^{h(L)} (\mathrm{i}\mu')^{h(L')} \mathscr{J}_L \mathscr{J}^*_{L'} \sum_{M=-L}^{L} \frac{[k_\mathrm{u}][k_\mathrm{l}][J_\mathrm{u}][K]}{[J_\mathrm{l}][L]} \\ \times (-1)^{k_\mathrm{u}+K} C(L', K, L; M', -Q, M) \begin{Bmatrix} J_\mathrm{u} & k_\mathrm{u} & J_\mathrm{u} \\ J_\mathrm{l} & k_\mathrm{l} & J_\mathrm{l} \\ L' & K & L \end{Bmatrix} \\ \times D^{L}_{M,\mu}(\phi_k, \theta_k, -\phi_k)^* D^{L'}_{M',\mu'}(\phi_k, \theta_k, -\phi_k),\end{aligned} \tag{13}$$

where $\{\}$ denotes the Wigner 9-j symbol [6]. The irreducible tensor of rank K constructed out of the two Fano statistical tensors is expressed in Eq. (12) using the short-hand notation

$$(t^{k_u}(i)\otimes t^{k_l}(f))^K_Q=\sum_{q_l} C(k_u,k_l,K;q_u,q_l,Q)t^{k_u}_{q_u}(i)t^{k_l}_{q_l}(f). \tag{14}$$

It may be noted that the above general result readily specializes to give the simple form of Eq. (56) of part I, when $J_u=1$ and $J_l=0$. Using the well-known Clebsch–Gordan theorem for the D matrices we may eliminate the sum over M and reduce the product of the two D matrices in Eq. (13) into a single D matrix element. Explicitly, we can make the replacement

$$\sum_{M=-L}^{L} C(L',K,L;M',-Q,M)D^L_{M\mu}(\phi_k,\theta_k,-\phi_k)^*D^{L'}_{M'\mu'}(\phi_k,\theta_k,-\phi_k)$$

$$=(-1)^{L'+Q-\mu}\frac{[L]}{[K]}C(L',L,K;\mu',-\mu,v)D^K_{Qv}(\phi_k,\theta_k,-\phi_k), \tag{15}$$

in Eq. (13) by the right-hand side. The Stokes parameters [7] I,Q,U,V are now readily expressed, following part I, by

$$S_0=I=\rho^{\gamma}_{+1,+1}(f,i)+\rho^{\gamma}_{-1,-1}(f,i),\quad S_1=Q=\rho^{\gamma}_{+1,-1}(f,i)+\rho^{\gamma}_{-1,+1}(f,i),$$

$$S_2=U=i\{\rho^{\gamma}_{+1,-1}(f,i)-\rho^{\gamma}_{-1,+1}(f,i)\},\quad S_3=V=\rho^{\gamma}_{+1,+1}(f,i)-\rho^{\gamma}_{-1,-1}(f,i), \tag{16}$$

in terms of the elements given by Eq. (12), which is the central result of this section. We note that $v=0$ in Eq. (15) for $S_0=I$, when

$$D^K_{Q0}(\phi_k,\theta_k,-\phi_k)=\sqrt{\frac{4\pi}{2K+1}}\,Y^*_{KQ}(\theta_k,\phi_k), \tag{17}$$

and hence the intensity can be expressed as a weighted sum of $Y_{KQ}(\theta_k,\phi_k)$ and the sum involves only those K which satisfy $(-1)^{L'+L-K}=1$. On the other hand, we note $v=0$ for $S_3=V$ as well so that the relation in Eq. (17) can be used. But it is important to note that $S_3=V$ is a weighted sum of $Y_{KQ}(\theta_k,\phi_k)$ for those K which satisfy $(-1)^{L'+L-K}=-1$. For $S_1=Q$ and $S_2=U$, we note that $v=\pm2$ and therefore K has necessarily to be $\geqslant 2$.

The Stokes parameters S_α $(\alpha=0,1,2,3)$ defined above may also be expressed using Eq. (9) in the form

$$S_\alpha=\sum_{m_u=-J_u}^{J_u}\sum_{m_l=-J_l}^{J_l}|c^i_{m_u}|^2|c^f_{m_l}|^2\mathscr{Z}_\alpha(m_l;m_u)$$

$$+\sum_{m_u\neq m'_u}\sum_{m_l\neq m'_l}\sum_{m'_u=-J_u}^{J_u}\sum_{m'_l=-J_l}^{J_l}c^i_{m_u}c^{i*}_{m'_u}c^{f*}_{m_l}c^f_{m'_l}\mathscr{C}_\alpha(m_l,m'_l;m_u,m'_u), \tag{18}$$

where the Stokes parameters $\mathscr{Z}_\alpha(m_l,m_u)$ for $\alpha=0,1,2,3$ for a pure Zeeman transition from $|J_u,m_u\rangle$ to $|J_l,m_l\rangle$ are readily expressible, following Eq. (16) as

$$\mathscr{Z}_0(m_l;m_u)=\mathscr{Z}_{+1,+1}(m_l;m_u)+\mathscr{Z}_{-1,-1}(m_l;m_u),$$

$$\mathscr{Z}_1(m_l;m_u)=\mathscr{Z}_{+1,-1}(m_l;m_u)+\mathscr{Z}_{-1,+1}(m_l;m_u),$$

$$\mathscr{Z}_2(m_l; m_u) = i[\mathscr{Z}_{+1,-1}(m_l; m_u) - \mathscr{Z}_{-1,+1}(m_l; m_u)],$$
$$\mathscr{Z}_3(m_l; m_u) = \mathscr{Z}_{+1,+1}(m_l; m_u) - \mathscr{Z}_{-1,-1}(m_l; m_u), \tag{19}$$

in terms of

$$\mathscr{Z}_{\mu,\mu'}(m_l; m_u) = p_i F(f, i; x) \sum_L \sum_{L'} (-i\mu)^{h(L)} (i\mu')^{h(L')} \mathscr{J}_L \mathscr{J}^*_{L'} \times C(J_l, L, J_u; m_l, M, m_u) C(J_l, L', J_u; m_l, M, m_u) \times D^L_{M,\mu}(\phi_k, \theta_k, -\phi_k)^* D^{L'}_{M,\mu'}(\phi_k, \theta_k, -\phi_k). \tag{20}$$

The first part of right-hand side in Eq. (18) is thus a statistically weighted sum of pure Zeeman contributions which we may refer to, for brevity, as Zeeman term.

Likewise, the $\mathscr{C}_\alpha(m_l, m'_l; m_u, m'_u)$ can be expressed as

$$\mathscr{C}_0(m_l, m'_l; m_u, m'_u) = \mathscr{C}_{+1,+1}(m_l, m'_l; m_u, m'_u) + \mathscr{C}_{-1,-1}(m_l, m'_l; m_u, m'_u),$$
$$\mathscr{C}_1(m_l, m'_l; m_u, m'_u) = \mathscr{C}_{+1,-1}(m_l, m'_l; m_u, m'_u) + \mathscr{C}_{-1,+1}(m_l, m'_l; m_u, m'_u),$$
$$\mathscr{C}_2(m_l, m'_l; m_u, m'_u) = i[\mathscr{C}_{+1,-1}(m_l, m'_l; m_u, m'_u) - \mathscr{C}_{-1,+1}(m_l, m'_l; m_u, m'_u)],$$
$$\mathscr{C}_3(m_l, m'_l; m_u, m'_u) = \mathscr{C}_{+1,+1}(m_l, m'_l; m_u, m'_u) - \mathscr{C}_{-1,-1}(m_l, m'_l; m_u, m'_u), \tag{21}$$

in terms of

$$\mathscr{C}_{\mu,\mu'}(m_l; m'_l; m_u, m'_u) = p_i F(f, i; x) \sum_L \sum_{L'} (-i\mu)^{h(L)} (i\mu')^{h(L')} \mathscr{J}_L \mathscr{J}^*_{L'} C(J_l, L, J_u; m_l, M, m_u) C(J_l, L', J_u; m'_l, M', m'_u) D^L_{M,\mu}(\phi_k, \theta_k, -\phi_k)^* D^{L'}_{M',\mu'}(\phi_k, \theta_k, -\phi_k). \tag{22}$$

Clearly, the $\mathscr{C}_\alpha$ denote the contributions to the Stokes parameters from the cross-terms which arise due to quantum interference effects. The second part of Eq. (18) may be referred to, for brevity, as cross-term contributions.

3. Polarization of spin-1 and spin-$\frac{3}{2}$ atomic levels in the presence of combined external electric and magnetic fields

Using the same notations as in part I, the interaction Hamiltonian H_{int} for the case of an atomic level with spin J is given by [8]

$$H_{\text{int}} = \mathbf{D} \cdot \mathbf{J} + A[3J_z^2 - J(J+1) + \eta(J_x^2 - J_y^2)], \tag{23}$$

when the atom is exposed to an electric quadrupole field characterized by the parameters

$$A = \frac{QV_{zz}}{4J(2J-1)}, \quad \eta = \frac{V_{xx} - V_{yy}}{V_{zz}}, \tag{24}$$

satisfying $|V_{zz}| \geqslant |V_{xx}| \geqslant |V_{yy}|$ in the PAF of the electric quadrupole field and an arbitrarily oriented magnetic field **B** such that $\mathbf{D} = -g\mathbf{B}$, with g being the gyromagnetic ratio.

3.1. The case of $J = 1$

For $J = 1$, the interaction Hamiltonian given by Eq. (23) assumes the 3×3 matrix form

$$H_{\text{int}} = \begin{pmatrix} A + D_z & D_- & \eta A \\ D_+ & -2A & D_- \\ \eta A & D_+ & A - D_z \end{pmatrix}, \tag{25}$$

where the rows and columns are labeled by $|1,+1\rangle, |1,0\rangle$ and $|1,-1\rangle$ states in that order, defined with respect to the Z-axis of PAF, and the parameters $D_\pm = \frac{1}{\sqrt{2}}(D_x \pm \mathrm{i}D_y)$, in terms of the components (D_x, D_y, D_z) of **D** with respect to the PAF.

In the absence of a magnetic field (i.e., $\mathbf{D} = 0$), the energy eigen values and the corresponding eigen states of Eq. (25) are easily determined. These energy eigen states of H_{int} are

$$|X\rangle = \frac{1}{\sqrt{2}}(|1,-1\rangle - |1,1\rangle), \quad |Y\rangle = \frac{1}{\sqrt{2}}(|1,-1\rangle + |1,1\rangle), \quad |Z\rangle = |1,0\rangle, \tag{26}$$

which correspond, respectively, to the energy eigen values

$$E_X = (1-\eta)A, \quad E_Y = (1+\eta)A, \quad E_Z = -2A. \tag{27}$$

When $\mathbf{D} \neq 0$, the matrix form of the interaction Hamiltonian H_{int} can be written, in terms of the $|X\rangle, |Y\rangle, |Z\rangle$ basis, as

$$H_{\text{int}} = \begin{pmatrix} E_X & -D_z & \mathrm{i}D_y \\ -D_z & E_Y & D_x \\ -\mathrm{i}D_y & D_x & E_Z \end{pmatrix}. \tag{28}$$

The particularly simple case where **B** is along the Z-axis of PAF was discussed in part I, when Eq. (25) specializes to Eq. (21) of part I. There are two other geometries viz., where **B** is along the X-axis or along the Y-axis of PAF, when the secular equation for the determinant factors out into a product of linear and quadratic forms. We give below all these solutions.

3.1.1. Magnetic field **B** along the X-axis of PAF

If **B** is along the X-axis of the PAF, i.e., **D** has components $(D, 0, 0)$, the eigen states and eigen values are given by

$$|\Psi_1\rangle = \frac{(E_1 - E_Y)|Z\rangle + D|Y\rangle}{N_1}, \quad E_1 = \frac{[A(\eta-1) - \{A^2(3+\eta^2) + 4D^2\}^{1/2}]}{2}, \tag{29a}$$

$$|\Psi_2\rangle = \frac{D|Z\rangle + (E_2 - E_z)|Y\rangle}{N_2}, \quad E_2 = \frac{[A(\eta-1) + \{A^2(3+\eta^2) + 4D^2\}^{1/2}]}{2}, \tag{29b}$$

$$|\Psi_3\rangle = |X\rangle, \quad E_3 = A(1-\eta), \tag{29c}$$

where the normalization factors N_1 and N_2 are

$$N_1 = [(E_1 - E_Y)^2 + D^2]^{1/2}, \quad N_2 = [(E_2 - E_Z)^2 + D^2]^{1/2}. \tag{30}$$

3.1.2. Magnetic field **B** *along the Y-axis of PAF*

Likewise, when **B** is along the Y-axis of PAF, i.e., **D** has components $(0, D, 0)$, the eigen states and the eigen values are

$$|\Psi_1\rangle = \frac{(E_1 - E_X)|Z\rangle + \mathrm{i}D|X\rangle}{N_1}, \quad E_1 = \frac{[-A(\eta+1) - \{A^2(3-\eta^2) + 4D^2\}^{1/2}]}{2}, \tag{31a}$$

$$|\Psi_2\rangle = |Y\rangle, \quad E_2 = A(1+\eta), \tag{31b}$$

$$|\Psi_3\rangle = \frac{\mathrm{i}D|Z\rangle - (E_3 - E_Z)|X\rangle}{N_3}, \quad E_3 = \frac{[-A(\eta+1) + \{A^2(3-\eta^2) + 4D^2\}^{1/2}]}{2}, \tag{31c}$$

where the normalization factors are

$$N_1 = [(E_1 - E_X)^2 + D^2]^{1/2}, \quad N_3 = [(E_3 - E_Z)^2 + D^2]^{\frac{1}{2}}. \tag{32}$$

3.1.3. Magnetic field **B** *along the Z-axis of PAF*

If **B** is along the Z-axis of the PAF, i.e., **D** has components $(0, 0, D)$, the eigen states and eigen values are given by

$$|\Psi_1\rangle = |Z\rangle, \quad E_1 = -2A, \tag{33a}$$

$$|\Psi_2\rangle = \frac{(E_2 - E_X)|Y\rangle - D|X\rangle}{N_1}, \quad E_2 = A + \sqrt{A^2\eta^2 + D^2}, \tag{33b}$$

$$|\Psi_3\rangle = \frac{D|Y\rangle - (E_3 - E_Y)}{N_2}, \quad E_3 = A - \sqrt{A^2\eta^2 + D^2}, \tag{33c}$$

where the normalization factors N_1 and N_2 are

$$N_1 = [(E_2 - E_X)^2 + D^2]^{1/2}, \quad N_2 = [(E_3 - E_Y)^2 + D^2]^{1/2}. \tag{34}$$

We may note that the energy eigen states involve only the superposition of $|1,+1\rangle$ and $|1,-1\rangle$ states when the spin-1 state of the atom is experiencing either (i) a pure electric quadrupole field i.e., $\mathbf{D} = 0$ or (ii) a uniform magnetic field **B** along the Z-axis of the PAF together with the electric quadrupole field. It is worth noting that the energy eigen states in Sections 3.1.1 and 3.1.2 involve superposition of $|1,+1\rangle$ and $|1,-1\rangle$ together with $|1,0\rangle$ when the magnetic field is either along the X- or the Y-axis of the PAF.

3.1.4. Arbitrary orientation of **B** *with respect to the PAF*

In general, when the magnetic field is arbitrarily oriented with respect to the PAF, i.e., when **D** has all the three components D_x, D_y, D_z, the characteristic equation corresponding to Eq. (25) is

a cubic equation, which does not factor so easily. It is of the form [8,9]

$$E^3 - 3\mathscr{K}_1^2 E - 2\mathscr{K}_2 = 0, \tag{35}$$

where

$$\mathscr{K}_1 = \frac{1}{\sqrt{3}}[A^2(3+\eta^2) + D_x^2 + D_y^2 + D_z^2]^{1/2}, \tag{36a}$$

$$\mathscr{K}_2 = \frac{A}{2}[2A^2(\eta^2 - 1) + (2D_z^2 - D_x^2 - D_y^2) + \eta(D_x^2 - D_y^2)]. \tag{36b}$$

Comparison of Eq. (35) with the trigonometric identity $4\cos^3\Theta - 3\cos\Theta - \cos 3\Theta = 0$ leads to the eigen values

$$E_i = 2\mathscr{K}_1 \cos[\{\Theta + 2\pi(i-1)\}/3], \quad i = 1,2,3, \tag{37}$$

where $\Theta = \cos^{-1}[\mathscr{K}_2/\mathscr{K}_1^3]$. In Fig. 2 we have shown the splitting of energy levels as a function of θ_B and R, with $\phi_B = \pi/4$ for different values of asymmetry parameter η. The eigen states corresponding to E_i in Eq. (37) are

$$|\Psi_i\rangle = N[(-D_z D_x - \mathrm{i}\mathscr{R}_+ D_y)|X\rangle - (\mathrm{i}D_z D_y + \mathscr{R}_- D_x)|Y\rangle - (D_z^2 - \mathscr{R}_+\mathscr{R}_-)|Z\rangle], \tag{38}$$

where

$$\mathscr{R}_\pm = A(1 \pm \eta) - E_i, \tag{39}$$

and the normalization factor N is given by

$$N = [(\mathbf{D}\cdot\mathbf{D})D_z^2 + \mathscr{R}_+^2 D_y^2 + \mathscr{R}_-^2 D_x^2 - 2\mathscr{R}_+\mathscr{R}_- D_z^2 + \mathscr{R}_+^2\mathscr{R}_-^2]^{-1/2}. \tag{40}$$

Clearly, the eigen states $|\Psi_i\rangle$ given by Eq. (38) involve superposition of all the three states $|1,\pm1\rangle$ and $|1,0\rangle$ for an arbitrary orientation of the magnetic field. Using Eq. (26), we can express $|\Psi_i\rangle$ in terms of the $|J_\mathrm{u}, m_\mathrm{u}\rangle$ states in the form of Eq. (1) where it is clear that the $c^i_{m_\mathrm{u}}$ are not only functions of the ratio $R = B/A$ of the strengths of magnetic and electric fields but also the asymmetry parameter η and the angles (θ_B, ϕ_B) specifying the orientation of the magnetic field **B** with respect to PAF of the electric field.

The energy levels, E_i are shown in Fig. 2, as a function of θ_B and R, for fixed $\phi_B = \pi/4$ and for different values of η. We can see from Fig. 2 that the energy levels are non-degenerate and unequally spaced except when $\eta = 0$ and $\theta_B = 0$ or π. The position of the unperturbed level is identified by $B = A = 0$. The level E_1 is above $E = 0$ (the unperturbed level) and the level E_2 is below $E = 0$, for all values of θ_B, ϕ_B, η and R. We will show later that as a consequence of this, we see additional line components in the wings of the profile. However, the middle level E_3 could lie above or below $E = 0$, depending on the values of θ_B, ϕ_B, η and R. Further, the energy E_3 becomes identical with $E = 0$ for some values of these parameters. The energy level shifts depend strongly on the field strengths, as is evident from the lower panels in Fig. 2. Typical numerical values of the expansion coefficients $c^i_{m_\mathrm{u}}$ in Eq. (1) for $J_\mathrm{u} = 1$ are presented in Table 1, while Table 2 summarizes the extent of contributions to the wave functions $|\Psi_1\rangle, |\Psi_2\rangle$ and $|\Psi_3\rangle$ from the basis states $|1,\pm1\rangle$

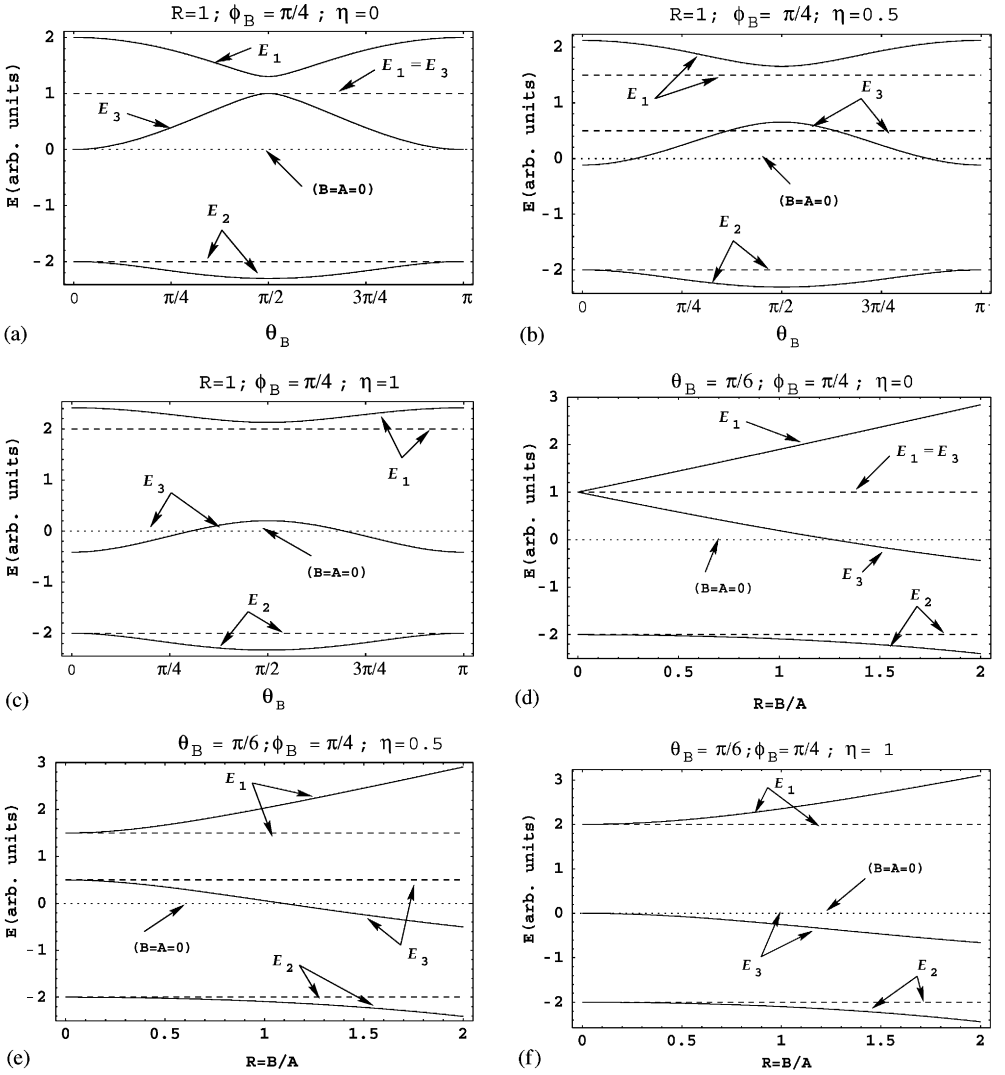

Fig. 2. The level splitting for $J_u = 1$ state in the presence of combined electric and magnetic fields. In panels (a)–(c) the solid lines represent the level splitting as a function θ_B, with fixed values of R and ϕ_B, for $\eta = 0, 0.5, 1$, respectively. In panels (d)–(f) the solid lines represent the level splitting as a function of R, with fixed values of θ_B and ϕ_B, for $\eta = 0, 0.5, 1$, respectively. In panels (a)–(f) the dotted line represents the unperturbed energy level corresponding to the absence of external electric and magnetic fields. The dashed lines represent the level splitting for the corresponding pure electric quadrupole field case. In this case, the levels E_1 and E_3 are degenerate only when $\eta = 0$. Moreover, the level E_3 coincides with the unperturbed energy level when $\eta = 1$.

and $|1, 0\rangle$, for chosen values of θ_B, ϕ_B, η and R. These contributions represented as probabilities $|c^i_{m_u}|^2$ for the basis states under consideration are displayed under the columns pertaining to the Zeeman terms. The cross-terms viz. $2\,\mathrm{Re}(c^i_{m_u} c^{i*}_{m'_u})$, which are representative of the quantum interference play a significant role in determining the Stokes line profiles.

Table 1
The expansion coefficients $c^i_{m_u}$ of the wave function $|\Psi_i\rangle$ for a transition $J_u = 1 \rightarrow J_l = 0$, using electric and magnetic field parameters $\eta = 1$, $R = B/A = 1$, $\theta_B = \pi/6$ and $\phi_B = \pi/4$

i	(m_u)		
	$+1$	0	-1
1	0.847−i0.321	−0.082+i0.0	0.391−i0.135
2	−0.038+i0.101	−0.978+i0.0	−0.092−i0.155
3	0.165+i0.373	0.193+i0.0	−0.301−i0.840

Table 2
Contributions arising from the Zeeman terms and cross-terms to the Stokes I, Q, U, V profiles for a transition $J_u = 1 \rightarrow J_l = 0$. The electric and magnetic field parameters employed are $\eta = 1$, $R = B/A = 1$, $\theta_B = \pi/6$ and $\phi_B = \pi/4$

Energy eigen state	Multiplying coefficient					
	Zeeman terms ($m_u = m'_u$)			Cross-terms ($m_u \neq m'_u$)		
	1	0	-1	1,−1	−1,0	1,0
$\|\Psi_1\rangle$	0.82	0.01	0.17	0.76	−0.06	−0.14
$\|\Psi_2\rangle$	0.01	0.96	0.03	−0.02	0.18	0.08
$\|\Psi_3\rangle$	0.16	0.04	0.80	−0.72	−0.12	0.06

3.2. The case of $J = \frac{3}{2}$

The interaction Hamiltonian H_{int} given by Eq. (23) assumes the form

$$H_{\text{int}} = \begin{pmatrix} 3A + \frac{3}{2}D_z & \sqrt{\frac{3}{2}}D_- & \sqrt{3}\eta A & 0 \\ \sqrt{\frac{3}{2}}D_+ & -3A + \frac{1}{2}D_z & \sqrt{2}D_- & \sqrt{3}\eta A \\ \sqrt{3}\eta A & \sqrt{2}D_+ & -3A - \frac{1}{2}D_z & \sqrt{\frac{3}{2}}D_- \\ 0 & \sqrt{3}\eta A & \sqrt{\frac{3}{2}}D_+ & 3A - \frac{3}{2}D_z \end{pmatrix}, \tag{41}$$

with respect to the basis states $|\frac{3}{2}, \frac{3}{2}\rangle, |\frac{3}{2}, \frac{1}{2}\rangle, |\frac{3}{2}, -\frac{1}{2}\rangle$ and $|\frac{3}{2}, -\frac{3}{2}\rangle$, defined with respect to the Z-axis of PAF.

3.2.1. Pure magnetic field

If $A = 0$ and the quantization axis is chosen parallel to the direction of magnetic field, the energy eigen states of H_{int} of Eq. (41) corresponds simply to the basis states $|\frac{3}{2}, m\rangle$ individually, with energy eigen values $E_m = -gBm$, respectively. This is the well-known Zeeman splitting with equal spacing between the $(2J + 1)$ levels.

3.2.2. Pure electric quadrupole field

In the case of pure quadrupole field, the above form Eq. (41) of H_{int} can be brought to the block diagonal form by a simple permutation [9] of its rows and columns, i.e.,

$$H_{\text{int}} = \begin{pmatrix} 3A & \sqrt{3}\eta A & 0 & 0 \\ \sqrt{3}\eta A & -3A & 0 & 0 \\ 0 & 0 & 3A & \sqrt{3}\eta A \\ 0 & 0 & \sqrt{3}\eta A & -3A \end{pmatrix}, \tag{42}$$

with respect to the basis states $|\frac{3}{2},\frac{3}{2}\rangle, |\frac{3}{2},-\frac{1}{2}\rangle, |\frac{3}{2},-\frac{3}{2}\rangle$ and $|\frac{3}{2},\frac{1}{2}\rangle$ in that order. The energy eigen values are readily obtained by solving the quadratic equation. The eigen states and the corresponding eigen values are given by

$$|\Psi_1\rangle = \sqrt{\frac{\lambda+3A}{2\lambda}}\left|\frac{3}{2},\frac{3}{2}\right\rangle + \sqrt{\frac{\lambda-3A}{2\lambda}}\left|\frac{3}{2},-\frac{1}{2}\right\rangle,\ E_1 = +\lambda\ , \tag{43a}$$

$$|\Psi_2\rangle = -\sqrt{\frac{\lambda-3A}{2\lambda}}\left|\frac{3}{2},\frac{3}{2}\right\rangle + \sqrt{\frac{\lambda+3A}{2\lambda}}\left|\frac{3}{2},-\frac{1}{2}\right\rangle,\ E_2 = -\lambda\ , \tag{43b}$$

$$|\Psi_3\rangle = \sqrt{\frac{\lambda-3A}{2\lambda}}\left|\frac{3}{2},\frac{1}{2}\right\rangle + \sqrt{\frac{\lambda+3A}{2\lambda}}\left|\frac{3}{2},-\frac{3}{2}\right\rangle,\ E_3 = +\lambda\ , \tag{43c}$$

$$|\Psi_4\rangle = \sqrt{\frac{\lambda+3A}{2\lambda}}\left|\frac{3}{2},\frac{1}{2}\right\rangle - \sqrt{\frac{\lambda-3A}{2\lambda}}\left|\frac{3}{2},-\frac{3}{2}\right\rangle,\ E_4 = -\lambda\ , \tag{43d}$$

where $\lambda = (9A^2 + 3\eta^2A^2)^{1/2}$. Clearly, the energy eigen values are degenerate. As before we describe three cases of orientation of the magnetic field **B** along the three principal axes of the PAF.

3.2.3. Magnetic field **B** *along the Z-axis of PAF*

If magnetic field **B** is along the Z-axis of PAF, the interaction Hamiltonian assumes once again a block diagonal form, given by

$$H_{\text{int}} = \begin{pmatrix} H_1 & 0 \\ 0 & H_2 \end{pmatrix}, \tag{44}$$

where the submatrices H_1 and H_2 are

$$H_1 = \begin{pmatrix} 3A + \frac{3}{2}D_z & \sqrt{3}\eta A \\ \sqrt{3}\eta A & -3A - \frac{1}{2}D_z \end{pmatrix}, \quad H_2 = \begin{pmatrix} 3A - \frac{3}{2}D_z & \sqrt{3}\eta A \\ \sqrt{3}\eta A & -3A + \frac{1}{2}D_z \end{pmatrix}. \tag{45}$$

By solving the concerned quadratic equations, the eigen states and the corresponding eigen values are obtained readily as

$$|\Psi_1\rangle = \sqrt{\frac{a_1+b_1}{2a_1}}\left|\frac{3}{2},\frac{3}{2}\right\rangle + \frac{c}{\sqrt{a_1(a_1+b_1)}}\left|\frac{3}{2},-\frac{1}{2}\right\rangle,\ E_1 = d + a_1\ , \tag{46a}$$

$$|\Psi_2\rangle = \frac{-c}{\sqrt{a_1(a_1+b_1)}}\left|\frac{3}{2},\frac{3}{2}\right\rangle + \sqrt{\frac{a_1+b_1}{2a_1}}\left|\frac{3}{2},-\frac{1}{2}\right\rangle,\ E_2 = d - a_1\ , \tag{46b}$$

$$|\Psi_3\rangle = \sqrt{\frac{a_2+b_2}{2a_2}}\left|\frac{3}{2},\frac{1}{2}\right\rangle + \frac{c}{\sqrt{a_2(a_2+b_2)}}\left|\frac{3}{2},-\frac{3}{2}\right\rangle,\ E_3 = -d + a_2\ , \tag{46c}$$

$$|\Psi_4\rangle = \frac{-c}{\sqrt{a_2(a_2+b_2)}}\left|\frac{3}{2},\frac{1}{2}\right\rangle + \sqrt{\frac{a_2+b_2}{2a_2}}\left|\frac{3}{2},-\frac{3}{2}\right\rangle,\ E_4 = -d - a_2\ , \tag{46d}$$

where

$$a_1 = \sqrt{(b_1)^2 + 2c^2}, \quad a_2 = \sqrt{(b_2)^2 + 2c^2}, \tag{47a}$$

$$b_1 = 3A + D_z, \quad b_2 = 3A - D_z, \tag{47b}$$

$$c = \sqrt{\frac{3}{2}}\,\eta A, \quad d = \frac{D_z}{2}. \tag{47c}$$

It may be noted here that the energies are non-degenerate.

3.2.4. *Magnetic field* **B** *along the X-axis of PAF*

When the magnetic field **B** is along the X-axis of PAF, the interaction Hamiltonian takes the form

$$H_{\text{int}} = \begin{pmatrix} 3A & \frac{\sqrt{3}}{2}D_x & \sqrt{3}\eta A & 0 \\ \frac{\sqrt{3}}{2}D_x & -3A & D_x & \sqrt{3}\eta A \\ \sqrt{3}\eta A & D_x & -3A & \frac{\sqrt{3}}{2}D_x \\ 0 & \sqrt{3}\eta A & \frac{\sqrt{3}}{2}D_x & 3A \end{pmatrix}. \tag{48}$$

It can be brought to a block diagonal form by a rotation $R(\pi, \pi/2, \pi)$ where $(\pi, \pi/2, \pi)$ are the Eulerian angles as defined by Rose [5]. Following the same procedure as explained in the previous section, the eigen vectors and the eigen values are obtained. They are of the same form as Eq. (46a–d) with a_1, a_2 given by Eq. (47a) and

$$b_1 = \tfrac{3}{2}A(\eta - 1) + D_x, \quad b_2 = \tfrac{3}{2}A(\eta - 1) - D_x, \tag{49a}$$

$$c = \frac{1}{4}\sqrt{\frac{3}{2}}A(3+\eta), \quad d = \frac{D_x}{2}. \tag{49b}$$

Clearly, the energies are once again non-degenerate.

3.2.5. Magnetic field **B** *along the Y-axis of PAF*

When the magnetic field **B** is along the Y-axis of PAF, the interaction Hamiltonian assumes the form

$$H_{\text{int}} = \begin{pmatrix} 3A & -\mathrm{i}\frac{\sqrt{3}}{2}D_y & \sqrt{3}\eta A & 0 \\ \mathrm{i}\frac{\sqrt{3}}{2}D_y & -3A & -\mathrm{i}D_y & \sqrt{3}\eta A \\ \sqrt{3}\eta A & \mathrm{i}D_y & -3A & -\mathrm{i}\frac{\sqrt{3}}{2}D_y \\ 0 & \sqrt{3}\eta A & \mathrm{i}\frac{\sqrt{3}}{2}D_y & 3A \end{pmatrix}. \tag{50}$$

As before we make a rotation $R(0, \pi/2, \pi/2)$ and a simple permutation so that H_{int} can be brought into a block diagonal form. The eigen vectors and eigen values are once again given by Eq. (46a)–(d) with a_1, a_2 given by Eq. (47a) and

$$b_1 = -\tfrac{3}{2}A(\eta + 1) + D_y, \quad b_2 = -\tfrac{3}{2}A(\eta + 1) - D_y, \tag{51a}$$

$$c = \frac{1}{4}\sqrt{\frac{3}{2}}A(3 - \eta), \quad d = \frac{D_y}{2}. \tag{51b}$$

The energies are non-degenerate.

3.2.6. Arbitrary orientation of the magnetic field

For a general orientation of the magnetic field **B** the matrix representation of interaction Hamiltonian, given by Eq. (41) leads to a quartic secular equation

$$E^4 - pE^2 - qE - r = 0, \tag{52}$$

where

$$\begin{aligned} &p = 2(1 + \eta^2/3 + 5\zeta^2), \quad \zeta = gB/6A, \\ &q = 8\zeta^2(2 - 3\sin^2\theta + \eta\sin^2\theta\cos 2\phi) = 8\zeta^2 F(\eta, \theta, \phi), \\ &r = (-p^2/4) + 4\zeta^2[4\zeta^2 + \eta^2/3 - \{2F(\eta, \theta, \phi) - G(\eta, \theta)\}], \\ &G(\eta, \theta) = 9\cos^2\theta + \eta^2\sin^2\theta. \end{aligned} \tag{53}$$

The problem was solved by Muha [10] to give the eigen values

$$\begin{aligned} &E_1 = \tfrac{1}{2}[u_0^{1/2} + u_1^{1/2} + u_2^{1/2}], \quad E_2 = \tfrac{1}{2}[u_0^{1/2} - u_1^{1/2} - u_2^{1/2}], \\ &E_3 = \tfrac{1}{2}[-u_0^{1/2} - u_1^{1/2} + u_2^{1/2}], \quad E_4 = \tfrac{1}{2}[-u_0^{1/2} + u_1^{1/2} - u_2^{1/2}], \end{aligned} \tag{54}$$

with

$$\begin{aligned} &u_n = 2p/3 + \mathscr{R}\cos[(\delta + 2\pi n)/3], \quad n = 0, 1, 2, \\ &\mathscr{R} = 2/3(p^2 - 12r)^{1/2}, \quad \delta = \cos^{-1}\mathscr{C}, \\ &\mathscr{C} = \frac{4[q^2 - (2/27)p^3 - (8/3)pr]}{\mathscr{R}^3}. \end{aligned} \tag{55}$$

Table 3
The expansion coefficients $c^i_{m_u}$ of the wave function $|\Psi_i\rangle$ for a transition $J_u = \frac{3}{2} \rightarrow J_l = \frac{1}{2}$, using electric and magnetic field parameters $\eta = 1$, $R = B/A = 1$, $\theta_B = \pi/6$ and $\phi_B = \pi/4$

i	(m_u)			
	$+\frac{3}{2}$	$+\frac{1}{2}$	$-\frac{3}{2}$	$-\frac{1}{2}$
1	0.075−i0.066	0.939+i0.0	0.293−i0.187	0.127+i0.002
2	0.563−i0.433	0.588+i0.0	0.246−i0.157	0.255+i0.008
3	−0.050+i0.079	0.885+i0.0	0.169−i0.038	−0.184+i0.009
4	−0.040+i0.051	0.922+i0.0	0.197−i0.302	−0.126+i0.003

Table 4
Contributions arising from the Zeeman terms and cross-terms to the Stokes I, Q, U, V profiles for a transition $J_u = \frac{3}{2} \rightarrow J_l = \frac{1}{2}$. The electric and magnetic field parameters employed are $\eta = 1$, $R = B/A = 1$, $\theta_B = \pi/6$ and $\phi_B = \pi/4$ with $m_l = m'_l = \pm\frac{1}{2}$

Energy eigen state	Multiplying coefficient								
	Zeeman terms $(m_u = m'_u)$				Cross-terms $(m_u \neq m'_u)$				
	$(m_l = m'_l = \pm\frac{1}{2})$				$(m_l = m'_l = \frac{1}{2})$		$(m_l = m'_l = \pm\frac{1}{2})$	$(m_l = m'_l = -\frac{1}{2})$	
	$\frac{3}{2}$	$\frac{1}{2}$	$-\frac{1}{2}$	$-\frac{3}{2}$	$\frac{3}{2},\frac{1}{2}$	$\frac{3}{2},-\frac{1}{2}$	$\frac{1}{2},-\frac{1}{2}$	$\frac{1}{2},-\frac{3}{2}$	$-\frac{1}{2},-\frac{3}{2}$
$\|\Psi_1\rangle$	0.01	0.88	0.09	0.02	0.14	0.06	0.45	0.24	0.06
$\|\Psi_2\rangle$	0.50	0.35	0.09	0.06	0.66	0.41	0.29	0.30	0.12
$\|\Psi_3\rangle$	0.01	0.78	0.18	0.03	−0.09	−0.08	0.30	−0.33	−0.69
$\|\Psi_4\rangle$	0.00	0.85	0.13	0.02	−0.07	−0.05	0.36	−0.23	−0.05

Although Muha [10] has given algebraic expressions for the eigen states $|\Psi_i\rangle$ corresponding to the above energy values, we found that it is much easier to generate the states numerically using Mathematica to determine the coefficients $c^i_{m_u} = \langle \frac{3}{2}, m_u | \Psi_i \rangle$, $m_u = \frac{3}{2}, \ldots, -\frac{3}{2}$. The numerical values of $c^i_{m_u}$ are shown in Table 3 for a particular choice of electric and magnetic field parameters. These values are used in our numerical computations, the results of which are presented in the next section. For the lower level with $J_l = \frac{1}{2}$, the splitting is purely due to the magnetic field, so that the energies corresponding to the eigen functions are $-gBm$, with $m = \pm\frac{1}{2}$.

The energy levels E_i as a function of θ_B and R for chosen values of $\phi_B = \pi/4$ and $\eta = 0, 0.5, 1$ are shown in Fig. 3. The energy levels are non-degenerate and unequally spaced about the unperturbed level identified by $B = A = 0$. We see that they vary with the orientation angle θ_B as well as with the ratio of relative field strengths R. The energy eigen states $|\Psi_i\rangle$ corresponding to these energy levels E_i are superposition of all the basis states $|\frac{3}{2}, \pm\frac{3}{2}\rangle$ and $|\frac{3}{2}, \pm\frac{1}{2}\rangle$. The contributions of basis states $|\frac{3}{2}, \pm\frac{3}{2}\rangle$ and $|\frac{3}{2}, \pm\frac{1}{2}\rangle$ in $|\Psi_i\rangle$ are shown in columns (3)–(6) of Table 4 for selected parameters $\theta_B = \pi/6$, $\phi_B = \pi/4$, $\eta = 1$ and $R = 1$. The cross-terms that lead to Stokes parameters I, Q, U and V (see Eq. (18)) are shown in columns (7)–(11) of Table 4.

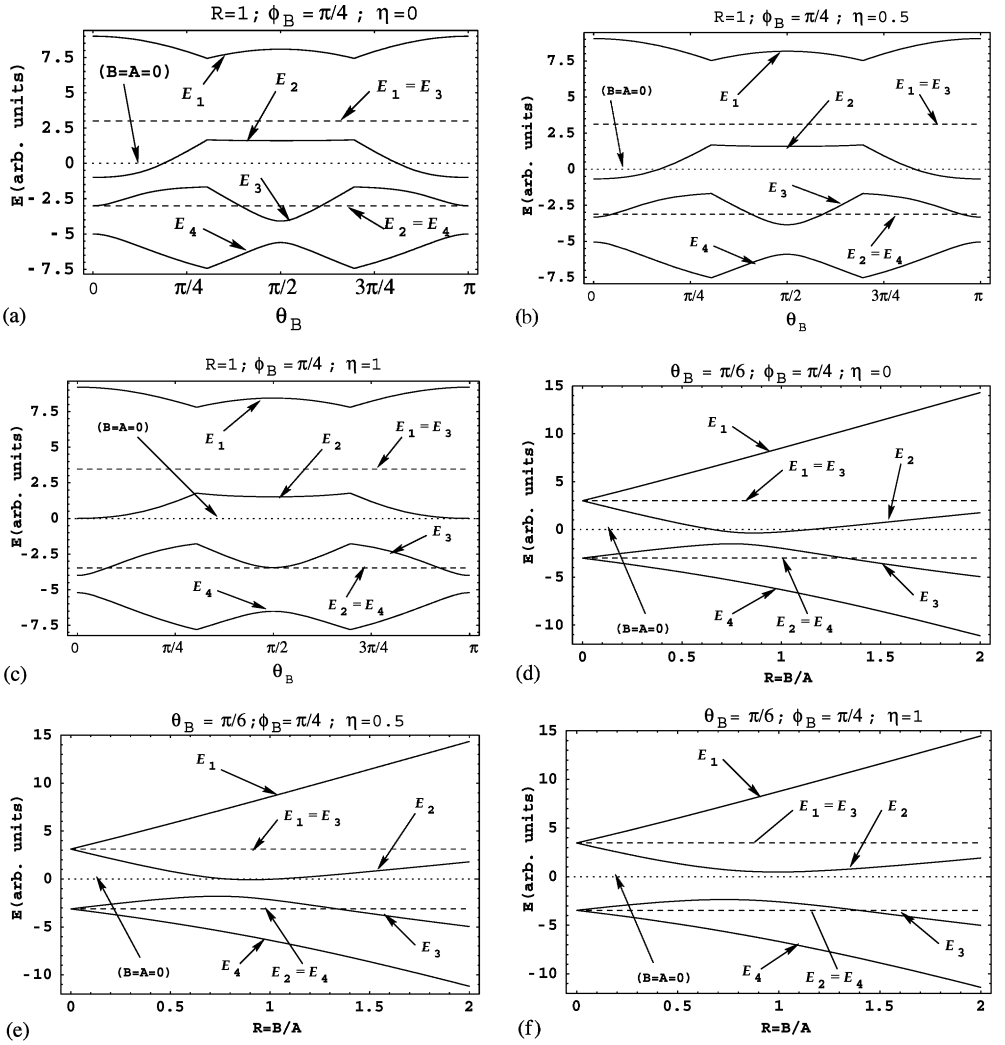

Fig. 3. The level splitting for $J_u = \frac{3}{2}$ state in the presence of combined electric and magnetic fields. In panels (a)–(c) the solid lines represent the level splitting as a function of θ_B, with fixed values of R and ϕ_B, for $\eta = 0, 0.5, 1$, respectively. In panels (d)–(f) the solid lines represent the level splitting as a function of R, with fixed values of θ_B and ϕ_B, for $\eta = 0, 0.5, 1$, respectively. In panels (a)–(f) the dotted line represents the unperturbed energy level corresponding to the absence of external electric and magnetic fields. The dashed lines represent the level splitting for the corresponding pure electric quadrupole field case. In this case, the level $E_1(E_2)$ is degenerate with $E_3(E_4)$ for all values of η.

4. Results and discussion

4.1. The Stokes line profiles in the case of $J_u = 1 \rightarrow J_l = 0$ transitions

The characteristic Stokes line profiles formed in the presence of the pure electric quadrupole field were discussed in Section 5.2 of part I and those in the presence of both magnetic and electric

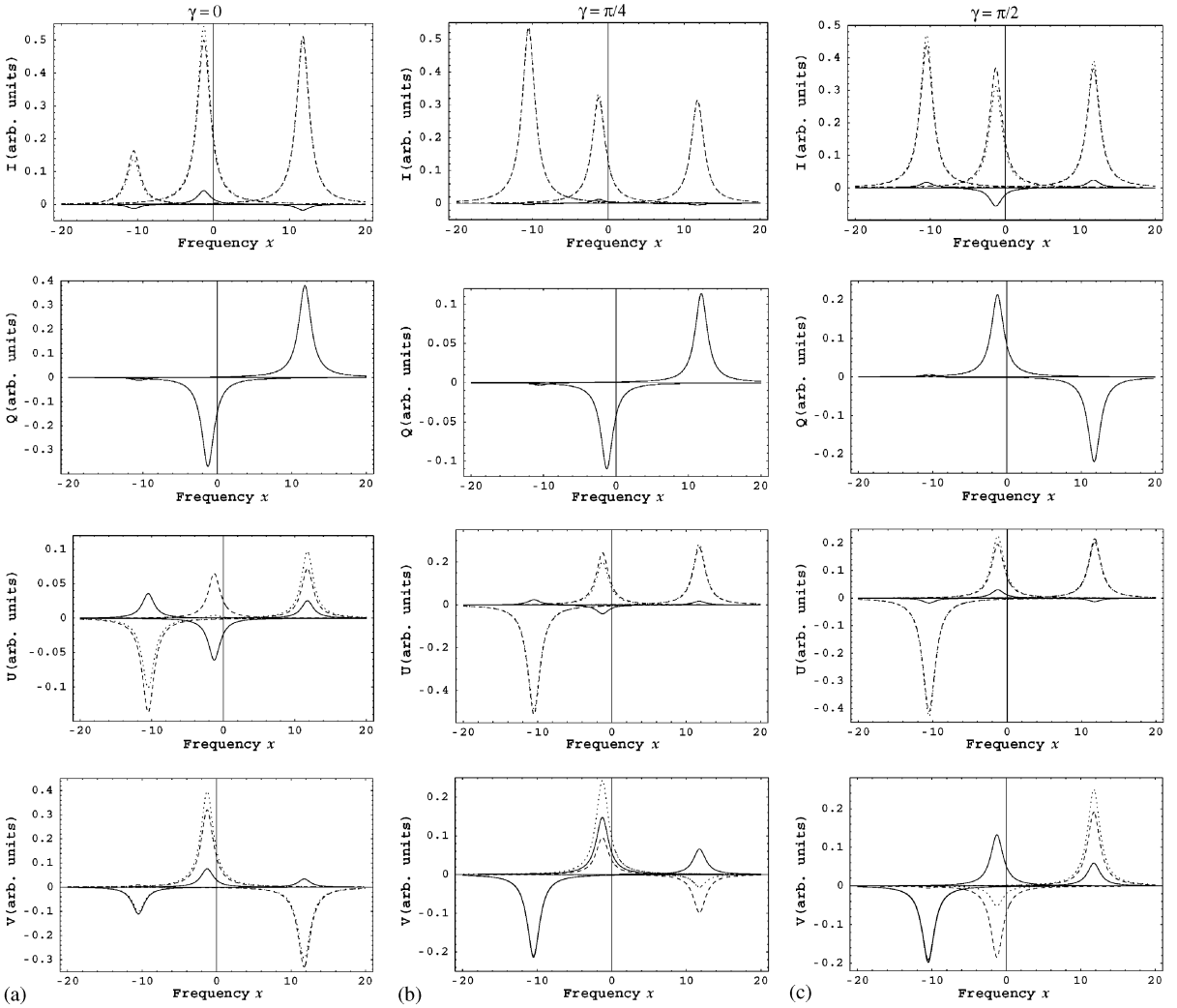

Fig. 4. The effect of combined electric quadrupole field and chosen direction of magnetic field $\theta_B = \pi/6, \phi_B = \pi/4$ and azimuth of the LOS $\phi_k = \pi/4$, on Stokes line profiles for $\eta = 1$ and $R = 1$. Panels (a)–(c) represent the emission Stokes line profiles of transition $J_u = 1 \rightarrow J_l = 0$ for different values of γ with assumed temperature $T = 6000$ K and natural line width $\Gamma = 2.18 \times 10^8$ s^{-1}. The three different curves (dashed, solid and dotted) correspond, respectively, to the Zeeman term contributions, cross-term contributions and the combined effect polarizations. The Stokes parameters I, Q, U and V are expressed in arbitrary units. The quantity $x = (\omega - \omega_0)/\Gamma$ is the frequency displacement from the line center in natural width units. The values $x > 0$ refer to the blue wing and $x < 0$ refer to the red wing of the line profile.

quadrupole fields (when magnetic field **B** is oriented along the Z-axis of the electric quadrupole field) were discussed in Section 5.3 of part I. For ready comparison, the Stokes line profiles formed in the presence of a pure magnetic field were also presented in Section 5.1 of part I.

We present in this paper the results for arbitrary orientations of the magnetic field. The Stokes line profiles are presented graphically in Fig. 4 for chosen values of $\eta = 1$ and $R = 1$. For convenience of

presentation, we choose a direction of magnetic field with $\theta_B = \pi/6$ and $\phi_B = \pi/4$. The azimuth angle of line of sight (LOS) is chosen to be $\phi_k = \pi/4$. With this choice the angle between the magnetic field direction and LOS direction becomes $\gamma = (\theta_B - \theta_k)$ where θ_k represents the orientation of the LOS (see Fig. 1).

In Fig. 4, we show the Stokes profiles arising due to contributions from the Zeeman term (dashed lines), cross-term (solid lines) and the general case of combined terms (dotted lines). We present the actual Stokes line profiles I, Q, U, V instead of the ratios $Q/I, U/I$ and V/I in order to theoretically establish the correspondence between the individual terms of Eq. (18) and the emergent Stokes line profiles. In the $\gamma = 0$ case (panel (a)), the Q Stokes parameter arises only due to the presence of electric quadrupole field (note that when $\gamma = 0$, the Q Stokes parameter vanishes in the pure Zeeman case). A similar effect is seen in the Stokes V profile also when $\gamma = \pi/2$ (magnetic field transverse to the LOS). For this chosen value of $\phi_B = \pi/4$, which highlights the contribution from cross-terms, one can see that the linear polarization (Q profile) arises only from these terms (pure Zeeman terms vanish for this value of ϕ_B). However, the Zeeman terms contribute to the linear polarization for other arbitrary choices of ϕ_B. The cross-term contributions in $|\Psi_1\rangle$ and $|\Psi_3\rangle$ lead to strong linear polarization components in the blue and near-red wings of the Q profiles, respectively. However, the cross-term contributions in $|\Psi_2\rangle$ lead to the appearance of a very weak linear polarization signal in the far-red wing. This fact is also readily seen by examining the magnitude of cross-term contributions as shown in Table 2. We have chosen $\phi_k = \pi/4$, in order to show the sensitivity of the Stokes U profiles to the physical parameters. Contributions arise from both Zeeman and cross-terms in the Stokes U profiles. In our earlier calculation Stokes V parameter for the pure Zeeman case revealed only two (left and right) circularly polarized components when $\gamma = 0$ [1]. In contrast, presently all the three circularly polarized components can be seen. This is a consequence of the superposition of all the concerned basis states (magnetic sub-states). The appearance of circularly polarized component (Stokes V profile) in the red wing is a consequence of the contribution of cross-terms. We notice that the effects of quadrupole electric field and magnetic field are comparable only when $R \sim 1$. For large values of R (say $R > 4$) the Zeeman effect dominates. Similarly, for $R < 1$ (say $R \sim 0.2$) the electric field effect dominates. Thus, we can consider $0.1 < R < 3$ as the sensitivity regime for quadrupole electric field effects on polarized line profiles.

4.2. The Stokes line profiles in the case of $J_u = \frac{3}{2} \to J_l = \frac{1}{2}$ transitions (taking only the dominant $L = 1$ contribution)

4.2.1. Pure magnetic field case

The results are presented graphically in Fig. 5 for the selected parameters $\theta_k = 0,\ \pi/4,\ \pi/2$ and $\phi_k = \pi/6$. In this case we present the ratio of emergent Stokes parameters $Q/I, U/I$ and V/I in order to provide a correspondence with the polarization measurements of the solar spectrum.

We know that a uniform magnetic field removes the degeneracy (Zeeman effect). Thus the magnetic field splits the upper $J_u = \frac{3}{2}$ level into four magnetic sub-levels and the lower $J_l = \frac{1}{2}$ level into two magnetic sub-levels, so that six transitions are possible between these split levels. The total number of transitions is determined by the selection rule ($\Delta m_J = 0, \pm 1$) of the transition, while the state of polarization is determined by the conservation of angular momentum, namely, Zeeman components with $\Delta m_J = \pm 1$ represent pairs of left and right circularly polarized radiation (σ lines) and $\Delta m_J = 0$ components represent plane polarized radiation (π lines). We can observe four σ lines

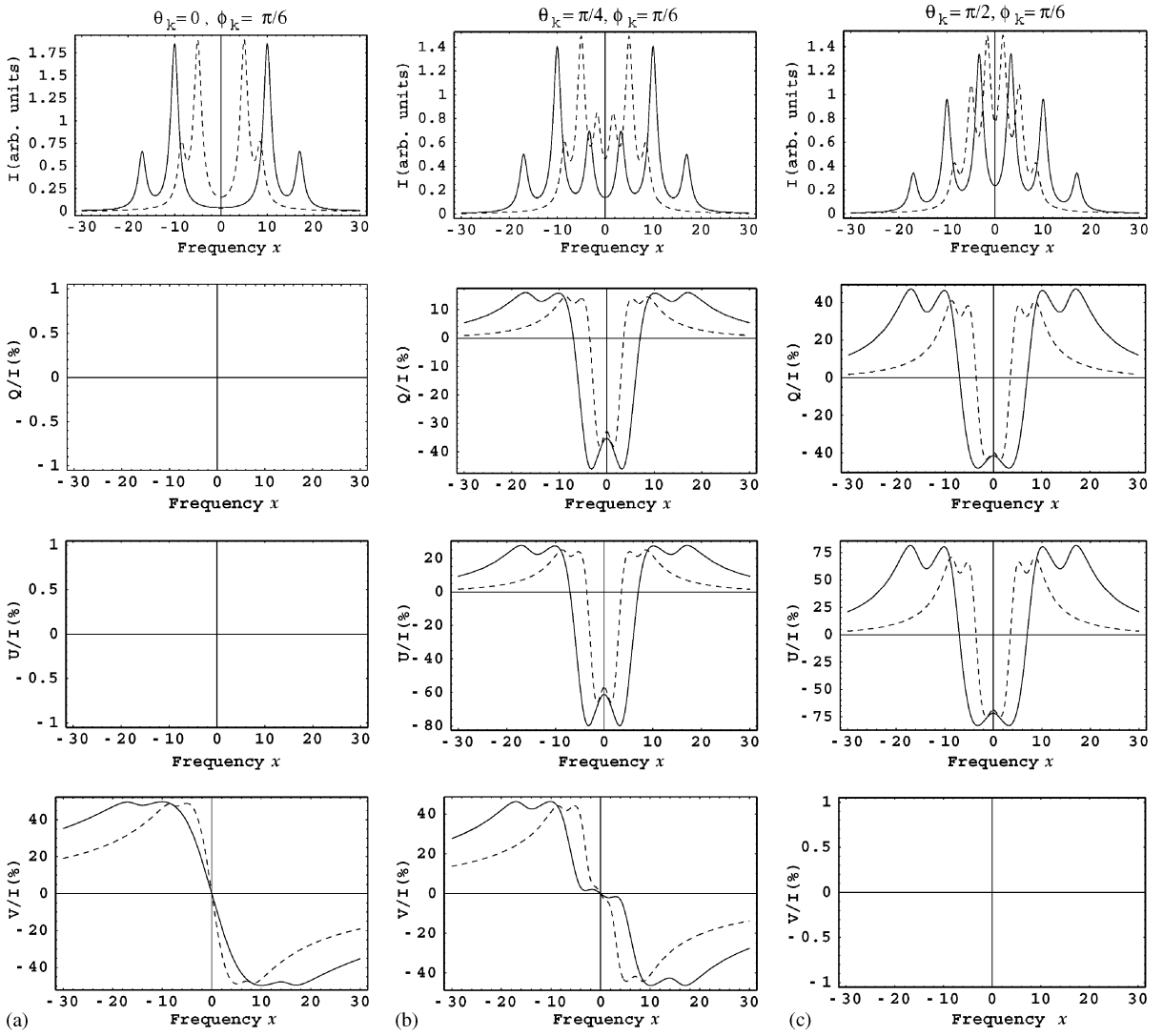

Fig. 5. The effect of pure magnetic field in the emission Stokes line profiles of transition $J_u = \frac{3}{2} \rightarrow J_l = \frac{1}{2}$ for a given temperature $T = 6000$ K and natural line width $\Gamma = 0.63 \times 10^8\ s^{-1}$. The dashed and solid curves correspond to two values (5,10, respectively) for the ratio of level splitting to natural line width. The percentage of linear and circular polarization ($Q/I, U/I$ and V/I profiles) are expressed in units of intensity. The quantity $x = (\omega - \omega_0)/\Gamma$ is the frequency displacement from the line center expressed in natural width units.

when the LOS is parallel to the quantization axis (magnetic field direction) and two π lines and four σ lines when the LOS is perpendicular to the quantization axis. They are symmetric around the line center. In linearly polarized Stokes Q/I and U/I profiles, the σ components appear in the blue and red line wings with a positive sign and the π components appear with a negative sign. The circularly polarized Stokes V/I profile is an antisymmetric line profile since the σ components in blue and red line wings have opposite signs.

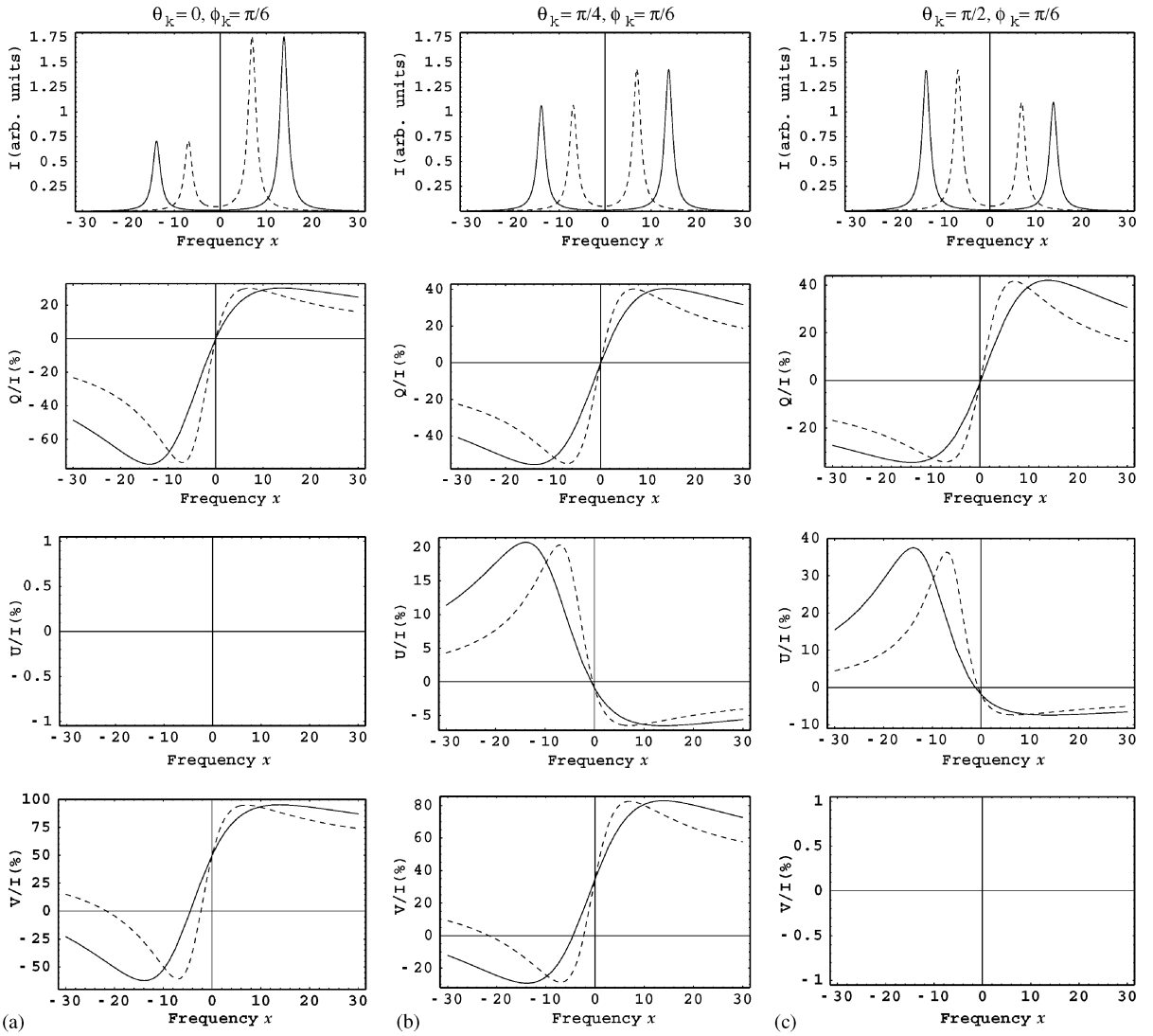

Fig. 6. The effect of pure electric quadrupole field ($\eta = 1$ case) in the emission Stokes line profiles for the transition $J_u = \frac{3}{2} \rightarrow J_l = \frac{1}{2}$ when the temperature $T = 6000$ K and natural line width $\Gamma = 0.63 \times 10^8$ s^{-1}. The dashed and solid curves correspond to two values (2,4, respectively) for the ratio of level splitting to natural line width. The percentage of linear and circular polarization ($Q/I, U/I$ and V/I profiles) are expressed in units of intensity. The quantity $x = (\omega - \omega_0)/\Gamma$ is the frequency displacement from the line center expressed in natural width units.

4.2.2. *Pure electric quadrupole field case*

The results are presented graphically in Fig. 6 for the selected parameters $\theta_k = 0,\ \pi/4, \pi/2$ and $\phi_k = \pi/6$. We present the emergent Stokes profiles $Q/I, U/I$ and V/I for a chosen asymmetry parameter $\eta = 1$.

In this case, the electric quadrupole field splits the upper $J_u = \frac{3}{2}$ level into four energy eigen states. One can see from Eqs. (43a–d) that each of two energy eigen states are degenerate. These

degenerate energy eigen states are superposition of basis states $|\frac{3}{2},\frac{3}{2}\rangle$ and $|\frac{3}{2},-\frac{1}{2}\rangle$, or superposition of $|\frac{3}{2},\frac{1}{2}\rangle$ and $|\frac{3}{2},-\frac{3}{2}\rangle$. We note that the energy levels corresponding to these energy eigen states are equally spaced and symmetric about the line center (see Fig. 3). These level spacings depend on electric field strength A and asymmetry parameter η. Increase in A and η results in increased spacing between these energy levels. However the lower $J_l = \frac{1}{2}$ level is unaffected by the electric quadrupole field. In the present calculation, we assume the lower energy eigen state is $|\frac{1}{2},\frac{1}{2}\rangle$. Thus only two transition components can be seen. The transition component arising from higher(lower) energy level appears in the blue(red) line wing. It is interesting to note that the difference in height of the emergent I profiles is caused by unequal superposition of basis states. As in the case of $J_u = 1 \rightarrow J_l = 0$ transition (see Fig. 9 of part I for comparison) the appearance of linear polarization Q/I profile even when the LOS is parallel to Z-axis of the PAF is a remarkable feature of the electric quadrupole field effect. In the present calculation ($J_u = \frac{3}{2} \rightarrow J_l = \frac{1}{2}$ transition), the V/I profile is non-zero (see panels (a) and (b)), because of unequal superposition of basis states. In contrast, in the previous calculation in part I ($J_u = 1 \rightarrow J_l = 0$ transition), the V/I profile always vanishes due to equal superposition of basis states (see Fig. 9 of part I for example). We do not show the results for the lower energy eigen state $|\frac{1}{2},-\frac{1}{2}\rangle$, because in that case V/I components simply change sign while Q/I and U/I profiles remain invariant with respect to the $|\frac{1}{2},\frac{1}{2}\rangle$ case discussed above.

4.2.3. *Combined electric quadrupole field and arbitrary orientation of magnetic field*

The theoretical results for this situation are presented in Fig. 7 for values of the free parameters given by $\eta = 1$ and $R = 1$. As in the Fig. 4, the magnetic field direction is again represented by $\theta_B = \pi/6$ and $\phi_B = \pi/4$. We confine the azimuth angle of LOS direction to $\phi_k = \pi/4$, so that the angle between the magnetic field direction and LOS direction is given by the relation $\gamma = \theta_B - \theta_k$ (see Fig. 1).

The combined effect of electric quadrupole field and arbitrarily oriented magnetic field is to split the upper $J_u = \frac{3}{2}$ level into four energy eigen states. However, the lower $J_l = \frac{1}{2}$ level is split into two non-degenerate energy eigen states due to external magnetic fields itself. Recall that the electric quadrupole field does not affect $J_l = \frac{1}{2}$ level. Thus, eight transition components can arise between the split levels. In this figure, we present the Stokes I, Q, U and V line profiles arising due to contributions from the Zeeman term, cross-term and the sum of these two (combined effects). As in the case of $J_u = 1 \rightarrow J_l = 0$ (see Fig. 4), Q profiles exclusively arise from the cross-terms. For the Stokes U and V parameters, both Zeeman and cross-terms contribute.

5. Conclusion

The quantum interferences between substates of different magnetic quantum numbers, discussed in this paper is qualitatively similar to the quantum interferences which are responsible for the well-known Hanle effect [11]. The quantum interferences in Hanle effect are due to the weakness of the magnetic field (when the splitting due to the magnetic field is small in comparison with the natural width arising due to the radiative damping of the concerned atomic state). That is, the separation between the $(2J + 1)$ magnetic substates within a given J level is so small that they overlap, resulting in partial degeneracy, and it would not be possible to uniquely specify the magnetic substate of a J level. The situation discussed in this paper, on the other hand, involves $(2J + 1)$

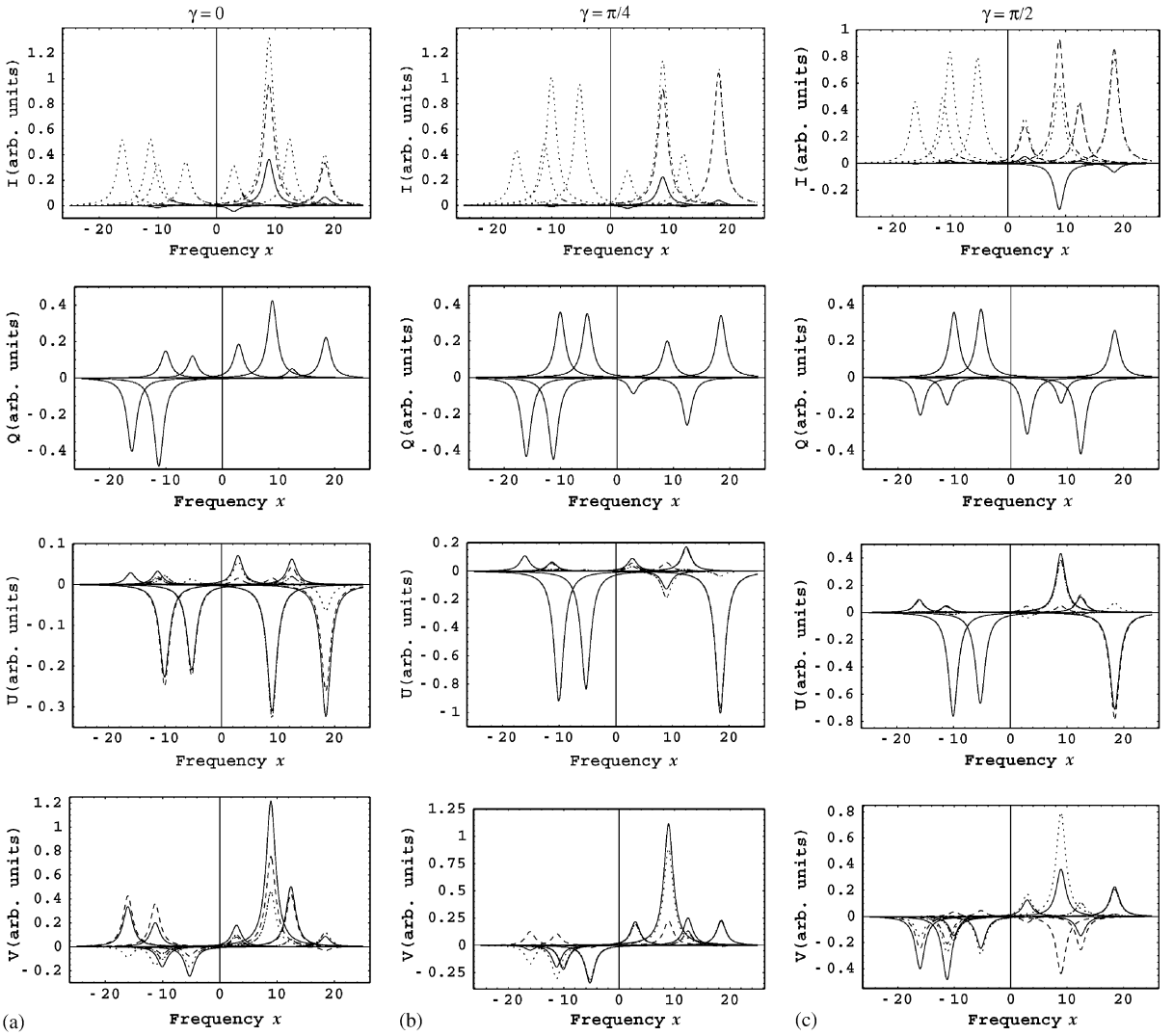

Fig. 7. The effect of combined electric quadrupole field (with $\eta = 1$) and the magnetic field (with $\theta_B = \pi/6, \phi_B = \pi/4$) on the Stokes line profiles for $\phi_k = \pi/4$ and $R = 1$. Panels (a)–(c) represent the emission Stokes line profiles for the transition $J_u = \frac{3}{2} \rightarrow J_l = \frac{1}{2}$ for different values of γ. A temperature of $T = 6000$ K and natural width $\Gamma = 0.63 \times 10^8$ s^{-1}. The dashed, solid and dotted curves correspond, respectively, to the Zeeman term contributions, cross-term contributions and the combined effect polarizations. The Stokes I, Q, U and V parameters are expressed in arbitrary units. The quantity $x = (\omega - \omega_0)/\Gamma$ is the frequency displacement from the line center expressed in natural width units.

energy levels which are well separated, i.e., the separations could be quite large compared to the natural widths. In the presence of an external electric quadrupole field, each of the $(2J + 1)$ energy levels is itself a superposition of $|J, m\rangle$ basis states, that can cause similar quantum interference effects. Whereas the Hanle effect demands the Zeeman splitting to be sufficiently weak, no such constraint on the external field strengths is necessary here. Note that the superposition of basis states

here is a result of electric quadrupole field effects and is independent of the magnetic field strength. In fact, the quantum interference effects are seen even when the magnetic field strength is zero. A careful measurement of the polarized second solar spectrum may reveal features present in the Stokes line profiles arising due to electric quadrupole fields, in addition to the magnetic fields. To the best of our knowledge, the models used until now for the analysis of line profiles only assume superposition of magnetic substates arising from the Hanle effect. It would be a worthwhile exercise, in our opinion, to look for features arising out of the presence of quadrupole electric fields in polarized Stokes profile measurements in solar and stellar atmospheres. We expect our calculations to provide a useful basis for interpreting such detailed measurements.

Acknowledgements

One of the authors (Y.Y.O.) wishes to express her gratitude to the Chairman, Department of Physics, Bangalore University and the Director, Indian Institute of Astrophysics (IIA), for providing the research facilities. She gratefully acknowledges Indian Council for Cultural Relations (ICCR), Ministry of External Affairs (MEA), Government of India, for awarding a scholarship. She also likes to thank Dr. P.N. Deepak for helpful discussions. Another author (G.R.) is grateful to Professor B.V. Sreekantan, Professor R. Cowsik and Professor J.H. Sastri for much encouragement and facilities provided for research at IIA.

References

[1] Yee Yee Oo, Nagendra KN, Sharath A, Vijayashankar R, Ramachandran G. Polarization of line radiation in the presence of external electric quadrupole and uniform magnetic fields. JQSRT, 2003, in press (this article is referred to as part I).
[2] Allen JE, Penn MJ, Michaels BP, Branston D, Ceja J. Polarization of the sodium D-lines in Mercury's atmosphere. American Astronomical Society/Division for Planetary Sciences Meeting, 2002.
[3] Stenflo JO, Nagendra KN. Solar polarization. Proceedings of the First SPW. Dordrecht: Kluwer Academic Publishers; l996 (also Solar Phys 1996, 164).
[4] Nagendra KN, Stenflo JO. Solar polarization. Proceedings of the Second SPW. Dordrecht: Kluwer Academic Publishers; 1999 (Astrophysics and Space Science Library ASSL 243).
[5] Rose ME. Elementary theory of angular momentum. New York: Wiley; 1957.
[6] Varshalovich DA, Moskalev AN, Khersonskii VK. Quantum theory of angular momentum. Singapore: World Scientific; 1988.
[7] Chandrasekhar S. Radiative transfer. Oxford: Clarendon Press; 1950.
[8] Muha GM. Exact solution of the NQR $I = 1$ eigenvalue problem for an arbitrary asymmetry parameter and Zeeman field strength and orientation. J Chem Phys 1980;73:4139–40.
[9] Swarnamala S. Theoretical studies on spin distributions in external electric and magnetic fields. PhD thesis, University of Mysore, India, 1995, unpublished.
[10] Muha GM. Exact solution of the eigenvalue problem for a spin-$\frac{3}{2}$ system in the presence of a magnetic field. J Magn Reson 1983;53:85–102.
[11] Moruzzi G, Strumia F. The Hanle effect and level-crossing spectroscopy. New York: Plenum Press; 1991.